Microstructural and Crystallographic Aspects of Thin Film Recording Media

David E. Laughlin, Bin Lu, Yu-Nu Hsu, Jie Zou, and David N. Lambeth

Abstract-- **Various aspects of the structure of thin film longitudinal recording media are presented and discussed. In particular we discuss the role that the various layers of thin film media play in controlling the microstructure and magnetic properties of the magnetic layer. These include the grain size of the films, the texture of the films, the role of the intermediate layer and the role of chemical segregation.**

***Index Terms*--epitaxy, magnetic recording media, microstructure, stacking faults, texture.**

I. Introduction

As the areal density of recording media increases it becomes more important to understand salient features of the microstructure of the recording media. In particular the size, orientation and perfection of the magnetic grains play an ever increasing role in determining the magnetic properties of thin film media.

II. Grain Size

The use of underlayers in magnetic media contributes to two important microstructural features of the magnetic layers, namely their grain size and their grain size distribution. In Figure 1 we show the microstructure of underlayers with three different textures. In Figure 1(a) the Cr film has the (110) texture and a grain size of about 25 nm. In Figure 1(b) the Cr film has the (002) texture and a grain size of about 24 nm. Figure 1(c) displays the NiAl film with a (112) texture and a grain size of about 14 nm. The grain size distributions of the (002) Cr in figure 1(b) and (112) NiAl in figure 1(c) are shown in figure 1 (d) and (e), respectively. The films displayed in Figure 1(a) and (c) were both deposited at room temperature, so the difference in their grain size is due to the inherently stronger bonding in the NiAl alloys. Since NiAl films have a smaller grain size than Cr films, when used as underlayers they produce Co alloy films with smaller grain sizes than Cr alloy underlayers [1] because of the epitaxial growth of the magnetic layers on them. Also, since the grain size distribution of the NiAl alloys is narrower than Cr underlayers, the resulting distribution of the magnetic grain size is also narrower, again, due to their epitaxial growth. These microstructural features play an important role on magnetic switching, coercivity, media noise and thermal stability.

III. Texture of The Underlayer

The underlayer texture used in longitudinal magnetic recording media has evolved over the last decade as follows:

$$(110)_{Cr} \Rightarrow (002)_{Cr} \Rightarrow (112)_{Cr/NiAl}$$

Each of these crystallographic textures gives rise to different textures of the magnetic films by means of epitaxy. Figure 2 shows electron diffraction patterns (EDPs) from (002) and (112) textured Cr and NiAl layers respectively. To understand these patterns it is important to remember that in high energy electron diffraction the wavelength of the incident electrons is much smaller (<0.004 nm) than the spacing of the crystalline planes to be examined. Thus we can approximate

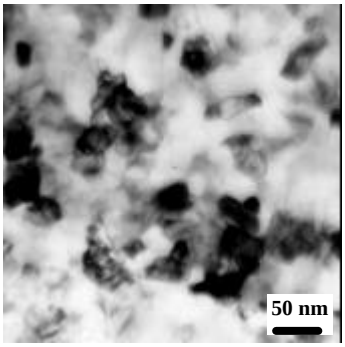

Figure 1 (a) (110) textured Cr film deposited at room temperature (RT) to a thickness of 100 nm

Manuscript received July 9, 1999. This work was supported in part by the *Data Storage System Center* at CMU (NSF ECD-8907068).

D. E. Laughlin is with the Materials Science and Engineering Department and the Data Storage Systems Center of Carnegie Mellon University, Pittsburgh PA, 15213, USA (dl0p@andrew.cmu.edu).

Bin Lu is with the Electrical and Computer Engineering Department and the Data Storage Systems Center of Carnegie Mellon University, Pittsburgh PA, 15213, USA (binlu@andrew.cmu.edu).

Yu-Nu Hsu is with the Materials Science and Engineering Department and the Data Storage Systems Center of Carnegie Mellon University, Pittsburgh PA, 15213, USA (yh2a@andrew.cmu.edu).

Jie Zou is with the Electrical and Computer Engineering Department and the Data Storage Systems Center of Carnegie Mellon University, Pittsburgh PA, 15213, USA (jzou@ece.cmu.edu).

David N. Lambeth is with the Electrical and Computer Engineering Department and the Data Storage Systems Center of Carnegie Mellon University, Pittsburgh PA, 15213, USA (lambeth@ece.cmu.edu).

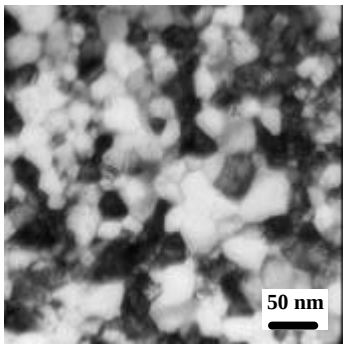

Figure 1 (b) (002) textured Cr film deposited at 250 ^{o}C to a thickness of 100 nm.

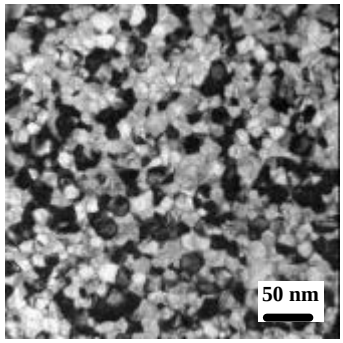

Figure 1 (c) (112) textured NiAl film deposited at RT to a thickness of 100 nm.

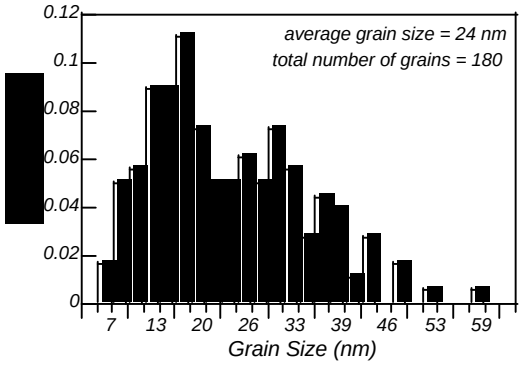

Figure 1 (d) grain size distribution of (002) Cr in Figure 1(b).

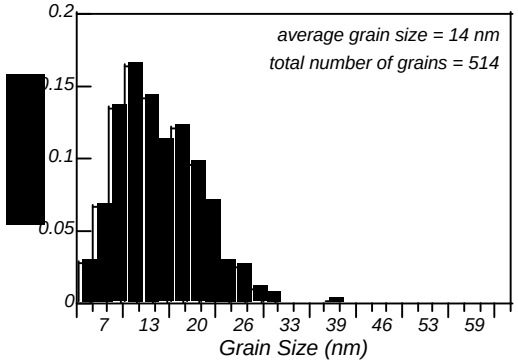

Figure 1 (e) grain size distribution of (112) NiAl in Figure 1(c).

the Bragg angle to be 0º, which means in transmission electron diffraction the only planes that can diffract are those which are *perpendicular* to the plane of the film. That is, the planes that diffract from an electron beam traveling in the [uvw] direction of a crystal are the planes of the [uvw] zone. When the texture is (002) the 112 ring (the third one) is missing (Figure 2a), since no {112} plane is perpendicular to the (002) plane. When the texture is (112), the 002 ring is missing (Fig. 1(b)) since no {002} plane is perpendicular to the (112) plane in a cubic material.

The fact that the rings are fairly continuous shows that the texture in both cases is random in the plane of the film. The degree of the texture can be obtained by tilting the samples as explained in detail in references [2,3]. Experiments [4,5] have shown that the $(110)_{Cr}$ and $(002)_{Cr}$ texture has a narrower angular distribution (±6°) than those of the $(112)_{NiAl}$ (±14°) and $(112)_{Cr/NiAl}$ (±10.6°).

Figure 3 shows a series of EDPs obtained at various tilting angles from a Cr (112) / NiAl (112) underlayer. The missing 002 ring in the zero tilt pattern (Figure 3(a)) demonstrates that the Cr film has a strong (112) texture. By observing at what angle the arcs appear as well as their length during tilting the angular distribution of the texture can be obtained. In this case it was found to be ±10.6° [4]

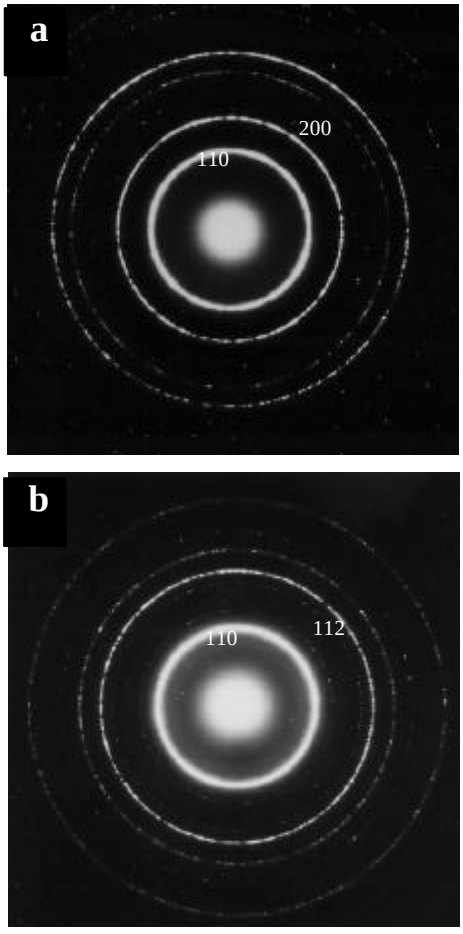

Figure 2 (a) EDP from (002) textured Cr layer. (b) EDP from (112) textured NiAl layer.

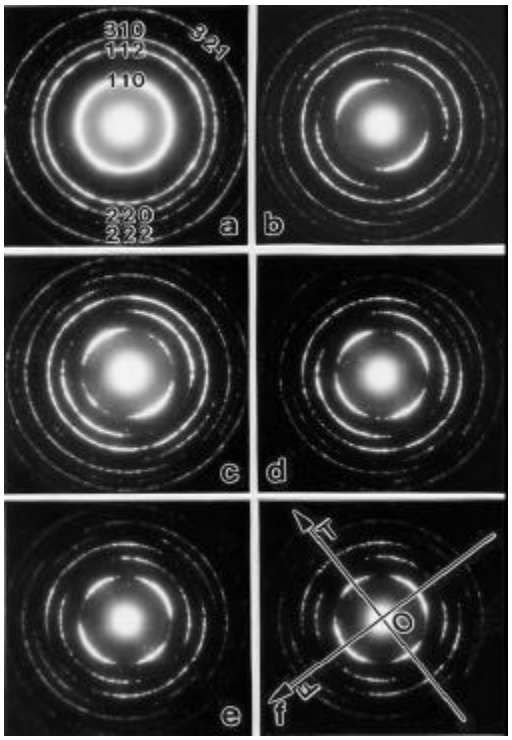

Figure 3 EDPs of the Cr layer of a Cr/NiAl/Al-Mg substrate film, deposited at room temperature. The EDPs are taken at different tilt angles around the tilt axis OT, a) 0°, b) 29°, c) 37°, d) 45°, e)52°, f) 55°.

X-ray diffraction from Cr/NiAl layers often show both the 110 and 112 reflections. The intensity of the 112 reflection increases when the Cr layer is added. Li *et al.* [6] and Lu *et al.* [4] suggest that this is because most of the (110) oriented NiAl grains are close to the NiAl film substrate interface. Figure 4 is a (110) dark field image of a cross section of a NiAl film. It shows that most of the grains with their (110) parallel to the film plane (the bright grains)) are close to the substrate film interface. This confirms the suggestion that the (112) texture increases with thickness in the NiAl films. It also explains why we do not see the 002 ring in the zero tilt EDP of the NiAl films (Figure 3(b)), since the TEM specimens were thinned from the substrate side.

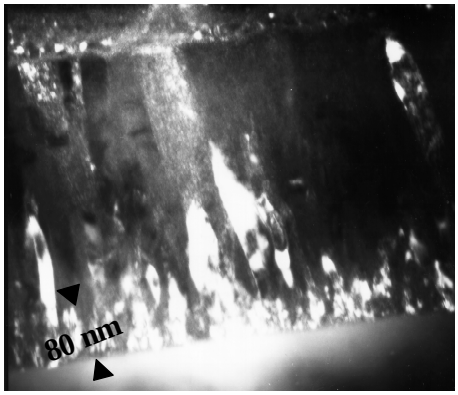

Figure 4 NiAl (110) Dark field image showing that most of the (110) oriented grains are near the film substrate interface.

IV. Texture of the Magnetic Layer

Figure 5 shows different textures of the Co alloy films grown on underlayers with different textures. Figure 5(a) is taken from a Co alloy that has been deposited on a Cr underlayer with a strong (002) texture. This is expected to give rise to the $(11\bar{2}0)$ texture through the following orientation relationship:

$$(11\bar{2}0)_{HCP} \;//\; (002)_{BCC}$$

The EDP shows most of the HCP rings to be present. The missing $11\bar{2}0$ ring shows that this film has a strong $(11\bar{2}0)$ texture. Figure 5(b) is taken from a Co alloy film that was deposited on a Cr/NiAl underlayer. This is expected to give rise to a $(10\bar{1}0)$ texture through the orientation relationship:

$$(10\bar{1}0)_{HCP} \;//\; (112)_{BCC}$$

The strong 0002 ring is indicative of a $(10\bar{1}0)$ texture. However the presence of weak $10\bar{1}0, 10\bar{1}1$ and $10\bar{1}2$ rings shows that there also exist randomly oriented grains. This has been reported previously [4,6].

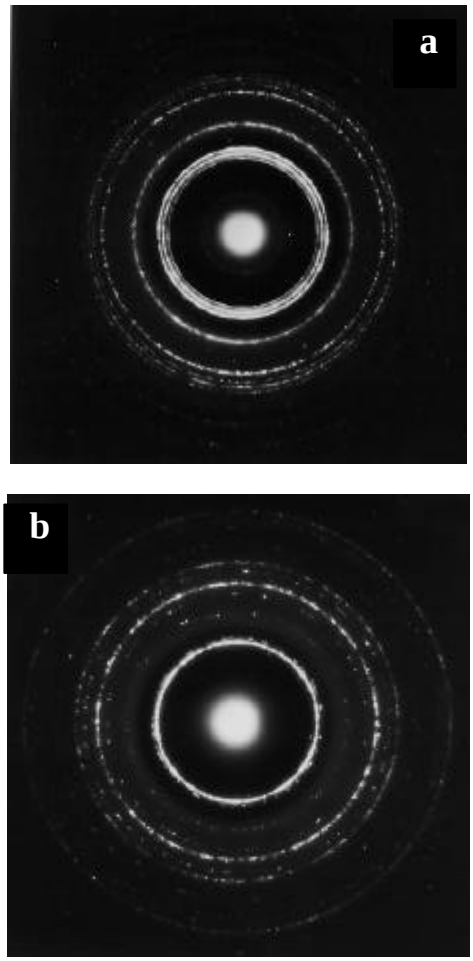

Figure 5 (a) EDP from a $(11\bar{2}0)$ textured Co film grown on (002) underlayer. (b) EDP from a $(10\bar{1}0)$ textured Co film grown on (112) Cr/NiAl underlayer.

Results from tilting experiments of the Co alloy films with the $(10\bar{1}0)$ texture are displayed in Figure 6. The angular distribution of the Co alloy grains have been shown to be about ±10.8° [4]. This is larger than the angular distribution of either the $(11\bar{2}0)$ or $(10\bar{1}0)$ textures of Co, where it was shown to be about ±6° [5].

V. Role of the Intermediate Cr Layer

It was first found by Lee *et al*. [7] that Co-alloy/Cr/NiAl films have much higher coercivites than Co-alloy/NiAl films. They showed that Co-alloy films grown on Cr intermediate layers had stronger $(10\bar{1}0)$ texture than those grown on NiAl. Moreover, the texture quality of Cr (112) is better than that of NiAl (112) texture [4].

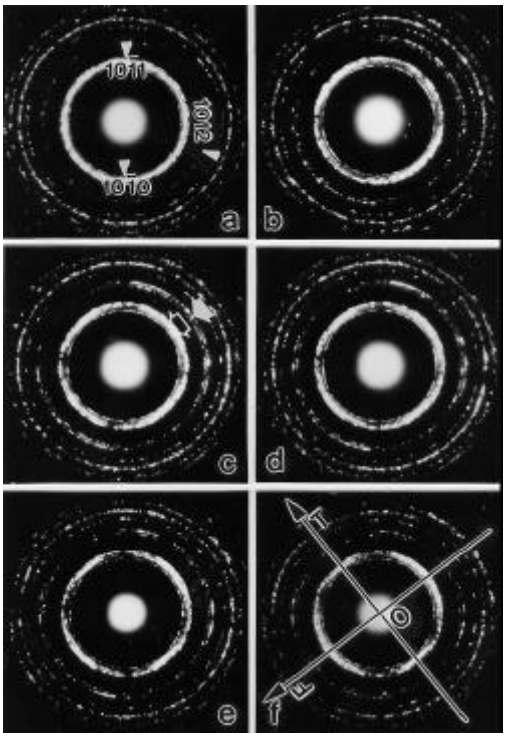

Figure 6 EDPs of the CoCrPtTa and Cr layers. The EDPs are taken at different tilt angles around the tilt axis OT, a) 0°, b) 29°, c) 38°, d) 41°, e)44°, f) 50°.

Figure 7 shows a $\sin(\omega_0/2)$ *vs.* $1/\sin b$ plot [2]. $\sin(\omega_0/2) = \sin\alpha/\sin\beta$, where, w_0 is the degree of the arc in the tilted EDP (see Figure 3 and 5), β is the tilting angle, a is the texture axis distribution angle. Therefore, the higher the slope of the line, the larger is α and the worse is the texture. It can be seen clearly that Cr and Co-alloy have better texture than the NiAl texture. The angular distribution of the Cr and Co-alloy layer is smaller than the NiAl layer by 4°.

We also found that there are more stacking faults in the Co-alloy/NiAl films than in the Co-alloy/Cr/NiAl thin films (See next section and Figure 9). The major role of the Cr intermediate layer is to decrease the stacking fault density of the magnetic layer by improving its own (112) texture (decreases α) and enhancing the epitaxial growth of Co-alloy. This consequently keeps the effective K_u from decreasing, which is important for high coercivity and high thermal stability of recorded bits [6].

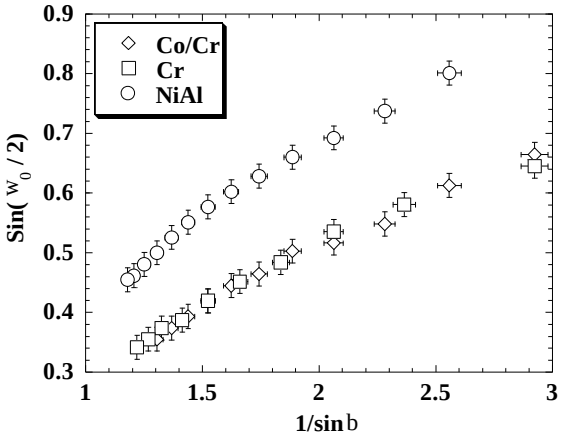

Figure 7 Plots of $\sin(\omega_0/2)$ vs. $1/\sin b$ of the CoCrPtTa/Cr, Cr, and NiAl layers in one sample. The texture axis distribution angle of the CoCrPtTa/Cr, Cr, and NiAl layers is determined as 10.8°, 10.6°, 14.4°, respectively.

VI. Stacking Faults in the Magnetic Layers

From the TEM bright images (Fig. 8(a) and (b)) it appears that $(11\bar{2}0)$ textured Co alloy films have more stacking faults than $(10\bar{1}0)$ textured films. However all stacking faults may not be observed in the bright field image of the $(10\bar{1}0)$ textured films because of the randomly oriented grains. Therefore electron diffraction has been carried out in order to obtain a better comparison. Fig. 9(a) shows the EDP of the Co-alloy $(11\bar{2}0)$ textured thin film. It can be seen clearly that there are many streaks on the $10\bar{1}1$ and $10\bar{1}2$ rings. The streaks have a fixed angle with their radial directions which are close to ± 61.9° for the $10\bar{1}1$ ring and ±43.1° for the $10\bar{1}2$ ring. These angles are those between the c axis and the $\{10\bar{1}1\}$ and $\{10\bar{1}2\}$ planes respectively.

Figure 9(b) shows the EDP of a Co-alloy /NiAl film. In this case, the streaks of $10\bar{1}1$ and $10\bar{1}2$ rings are in random directions and vary in length. Moreover, there are diffraction spots on either side of the rings. These features occur because of the randomly oriented grains. Streaks on $10\bar{1}1$ and $10\bar{1}2$ rings in the above mentioned directions come from grains that have their c-axis in the film plane. Grains that have their c-axis far from the film plane give rise to spots on either side of the rings because their streaks intersect the Ewald sphere. Grains whose c-axis are neither far from nor close to the film plane give randomly oriented streaks of varying lengths. It should be noted that the grains with $(10\bar{1}0)$ texture do not contribute to the $10\bar{1}1$ or $10\bar{1}2$ rings. At large tilting angles

we have not observed the streaks from $(10\bar{1}0)$ textured grains in the $10\bar{1}1$ and $10\bar{1}2$ arcs. This indicates that the $(10\bar{1}0)$ oriented Co grains have very low fault density. The reason why stacking faults are more prevalent in the $(11\bar{2}0)$ oriented grains than in the $(10\bar{1}0)$ oriented grains can be understood from the fact that there is more lattice mismatch in the former than the latter. In the Co-alloy $(11\bar{2}0)$ /Cr(002) case, the c-axis matches almost perfectly with a Cr <110> direction, while the other direction which is perpendicular to the c-axis has a 7% mismatch. This provides a shear stress in the (0002) planes, which forms stacking faults. In the Co-alloy $(10\bar{1}0)$ /Cr(112) /NiAl(112) case, the lattice is matched almost perfectly in both directions, thus there are no shear stresses to create stacking faults.

Figure 9c shows that with the addition of a Cr intermediate layer, the EDP has much fewer $10\bar{1}1$ and $10\bar{1}2$ streaks than without a Cr layer. This indicates that the intermediate layer significantly decreases the number of randomly oriented grains, thus decreasing the fault density.

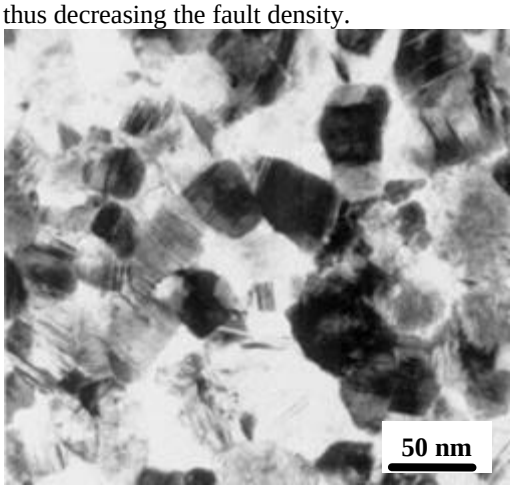

Figure 8 (a) TEM bright field image of CoCrTa with $(11\bar{2}0)$ texture on Cr with (002) texture.

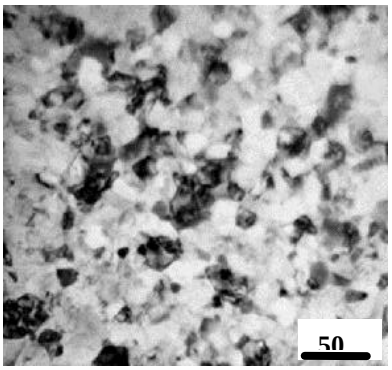

Figure 8 (b) TEM bright field image of CoCrPt with $(10\bar{1}0)$ texture on CrMn/NiAl with (112) texture.

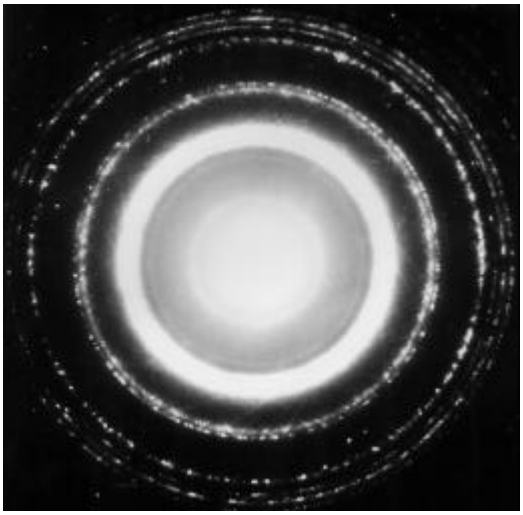

Figure 9 (a) EDP of CoCrTa with $(11\bar{2}0)$ texture on Cr with (002) texture.

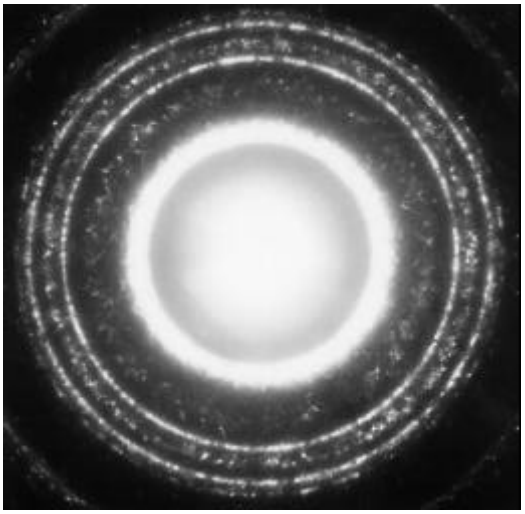

Figure 9 (b) EDP of CoCrPt with $(10\bar{1}0)$ texture on NiAl with (112) texture.

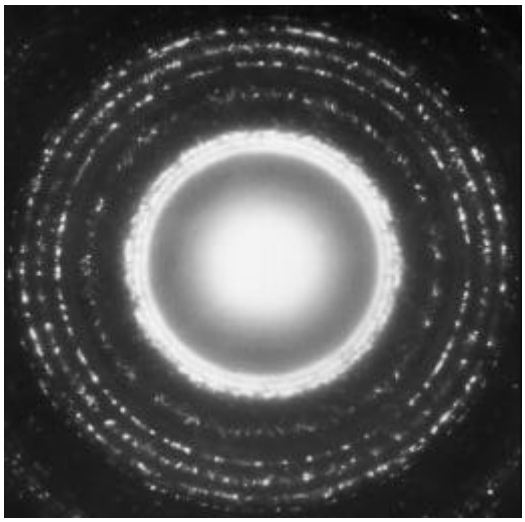

Figure 9 (c) EDP of CoCrPt with $(10\bar{1}0)$ texture on CrMn/NiAl with (112) texture.

VII. Chemical Segregation

A final feature of the films to be discussed is elemental segregation. Segregation can occur within the magnetic grains (intragranular) or at the grain boundaries of the magnetic films. The elemental segregation can occur either from within the magnetic grains themselves or from the underlayer or overlayer.

Segregation to the grain boundaries is thought to be a major contributor to the decrease in exchange coupling among the Co alloy grains. Exchange coupling among the Co grains plays a significant role in determining the magnetic and recording properties of Co-alloy thin films. A Co-alloy magnetic thin film with smaller exchange coupling usually has larger Hc, lower squareness and smaller media noise. Non-magnetic alloying elements, such as Cr, Mn, W and B, have been found to effectively reduce the exchange coupling in Co-based alloys as determined by δM and media noise measurements. On the other hand, while Pt significantly increases the magneto-crystalline anisotropy, it does not appear to reduce the exchange coupling between grains. This means that it probably does not segregate to the grain boundaries.

Compositional inhomogeneity in Co alloy recording media was first observed by Maedia *et al.* in 1985. They observed Cr segregation in CoCr thin films using TEM with selected-chemical-etching sample preparation [8]. Later, other techniques were utilized to analyze compositional inhomogeneity in the Co based alloys. These techniques include nano probe X-ray Energy Dispersive Spectroscopy (EDS)[9], nuclear magnetic resonance (NMR)[10], thermal magnetic analysis[11], ferromagnetic resonance (FMR)[12], atom probe field ion microscopy (APFIM)[13] and XAFS[14,15]. Each of these techniques have confirmed the existence of enriched Cr regions in the thin film which contribute to their magnetic properties. More recently Yahisa *et al.* [16] and Wittig *et al.* [17] have presented Co and Cr composition maps using energy-filtered TEM imaging. In their work the segregation of the Cr atoms to the Co alloy grain boundaries was directly observed by electron energy loss imaging.

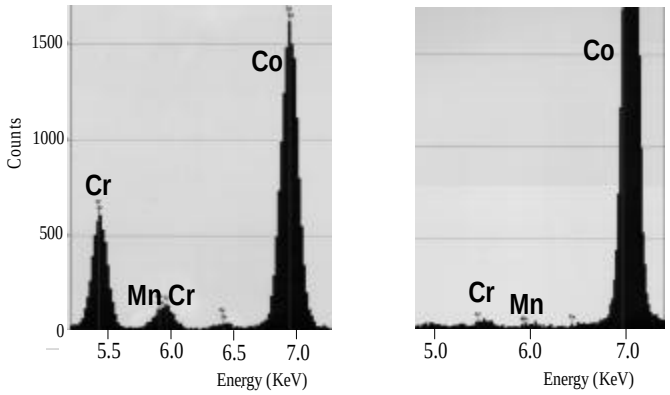

Figure 10 EDX spectra showing that both Cr and Mn atoms are present in greater amounts at the grain boundaries (a) of the Co film than in the center of the grains (b).

The Cr diffuses from the interiors of the grains to the grain boundaries and also may diffuse up the grain boundaries from the Cr based underlayer. To demonstrate that elements may diffuse up the Co grain boundaries from the underlayer we have deposited a pure Co film onto a CrMn underlayer. By means of EDX we have shown that the Cr and Mn at the grain boundaries of the Co films is much greater than that in the interior of the films. See Figure 10. Other elements such as Ta, Nb, B are believed to reduce the exchange coupling. It is not clear whether these or other elements actually segregate to the Co alloy grain boundaries or if they drive other alloying elements (such as Cr) to do so, which in turn provides for the magnetic isolation of the grains [18,19].

VIII. Acknowledgements

We thank the *Data Storage System Center* at CMU for financial support (NSF ECD-8907068). We also thank Mr. N. T. Nuhfer for assistance with the EDX.

IX. References

[1] L.-L. Lee, D. E. Laughlin and D.N. Lambeth, *IEEE Trans. Magn., MAG*-**30**, 3951 (1994).

[2] L. Tang and D.E. Laughlin, *Journal of Applied Crystallography* **29**, 411 (1996).

[3] B. Lu, L. Tang, D. N. Lambeth and D. E. Laughlin, "The Characterization of textures of Thin Films by Electron Diffraction", in Grain Growth in Polycrystalline Materials III", edited by H. Weiland, B. L. Adams and A. D. Rollett, TMS 1998.

[4] B. Lu, D.E. Laughlin, D.N. Lambeth, S.Z. Wu, R. Ranjan and G.C. Rauch, *J. Appl. Phys.* **85**, 4295 (1999).

[5] L. Tang, Y.C. Feng, L.-L. Lee and D.E. Laughlin, *Journal of Applied Crystallography* **29**, 419 (1996).

[6] J. Li, M. Mirzamaani, X. Bian, M. Doerner, S. Duan, K. Tang, M. Toney, T. Arnoldussen and M. Madison, *J. Appl. Phys*., **85,** 4286 (1999).

[7] Li-Lien Lee, David E. Laughlin, Leo Fang and David N. Lambeth, *IEEE Trans. Magn*., **31**, 2728 (1995).

[8] Y. Maeda, S. Hirono and M. Asahi, Japn. *J. Appl. Phys*., **24,** .L951 (1985).

[9] J. N. Chapman, I. R. McFadyen and J. P. C. Bernades, *J. Magn. Mag. Mater*., **62**, 359 (1986).

[10] K. Yoshida, H. Kakibayashi and H. Yasuoka, *J. Appl. Phys*., **68**, 705 (1990).

[11] Y. Maeda and M. Takahashi, *J. Appl. Phys*., **68**, 4751 (1990).

[12] J. B. C. Bernades, C. P. G. Schrauwen and H. W. Van Kesteren, *IEEE Trans. Magn.*, **26**, 33 (1990).

[13] K. Hono, Y. Maeda, J.-L. Li and T. Sakurai, *IEEE Trans. Magn*., **29**, 3745 (1993).

[14] K. M. Kemner, V. G. Harris, V. Chakarian, Y. U. Idzerda, W. T. Elam, C.-C. Kao, Y. C. Feng, D. E. Laughlin and J. C. Woicik, *J. Appl. Phys*., **79**, 5345 (1996).

[15] K. M. Kemner, V. G. Harris, W. T. Elam and C. J. Lodder, *IEEE Trans. Magn*., **30**, 4017 (1994).

[16] Y. Yahisa, K. Kimoto, K. Usami, Y. Matsuda, J. Inagak, K. Furusawa and S. Narishige, *IEEE Trans. Magn*., **31**, 2836 (1995).

[17] J. E. Wittig, T. P. Nolan, C. A. Ross, M. E. Schabes, K. Tang, R. Sinclair and J. Bentley, *IEEE Trans. Magn*., **34**, 1564 (1998).

[18] Y. Deng, D. N. Lambeth, and D. E. Laughlin, *IEEE Trans Magn*., **29**, 3676 (1993).

[19] Y. C. Feng, D. E. Laughlin and D. N. Lambeth, *IEEE Trans Magn*., **30,** 3948 (1994).